Slow development of bladder malfunction parallels spinal cord fiber sprouting and interneurons' loss after spinal cord transection

Sartori, Andrea M ; Hofer, Anna-Sophie ; Scheuber, Myriam I ; Rust, Ruslan ; Kessler, Thomas M ; Schwab, Martin E

Abstract: Neurogenic lower urinary tract dysfunction typically develops after spinal cord injury. We investigated the time course and the anatomical changes in the spinal cord that may be causing lower urinary tract symptoms following injury. Rats were implanted with a bladder catheter and external urethral sphincter electromyography electrodes. Animals underwent a large, incomplete spinal transection at the T8/9 spinal level. At 1, 2-3, and 4 weeks after injury, the animals underwent urodynamic investigations. Urodynamic investigations showed detrusor overactivity and detrusor-sphincter-dyssynergia appearing over time at 3-4 weeks after injury. Lower urinary tract dysfunction was accompanied by an increase in density of C-fiber afferents in the lumbosacral dorsal horn. CRF-positive Barrington's and 5-HT-positive bulbospinal projections drastically decreased after injury, with partial compensation for the CRF fibers at 3-4 weeks. Interestingly, a decrease over time was observed in the number of GABAergic neurons in the lumbosacral dorsal horn and lamina X, and a decrease of glutamatergic cells in the dorsal horn. Detrusor overactivity and detrusor-sphincter-dyssynergia might therefore arise from a discrepancy in inhibitory/excitatory interneuron activity in the lumbosacral cord as well as input changes which develop over time after injury. The processes point to spinal plastic changes leading to malfunction of the important physiological pathway of lower urinary tract control.

DOI: https://doi.org/10.1016/j.expneurol.2021.113937

Experimental Neurology 348 (2022) 113937

Contents lists available at ScienceDirect

Experimental Neurology

journal homepage: www.elsevier.com/locate/yexnr

Research Paper

Slow development of bladder malfunction parallels spinal cord fiber sprouting and interneurons' loss after spinal cord transection

Andrea M. Sartori [a,b,c,*,1], Anna-Sophie Hofer [a,c], Myriam I. Scheuber [a,c], Ruslan Rust [a,c], Thomas M. Kessler [b,2], Martin E. Schwab [a,c,2]

[a] Institute for Regenerative Medicine, University of Zürich, Switzerland
[b] Department of Neuro-Urology, Balgrist University Hospital, University of Zürich, Zürich, Switzerland
[c] Department of Health Sciences and Technology, ETH Zürich, Zürich, Switzerland

ARTICLE INFO

Keywords:
Spinal cord injury
Neurogenic lower urinary tract dysfunction (NLUTD)
C-fiber bladder afferents
Serotonin
Corticotropin-releasing factor
GABA
Interneurons

ABSTRACT

Neurogenic lower urinary tract dysfunction typically develops after spinal cord injury. We investigated the time course and the anatomical changes in the spinal cord that may be causing lower urinary tract symptoms following injury. Rats were implanted with a bladder catheter and external urethral sphincter electromyography electrodes. Animals underwent a large, incomplete spinal transection at the T8/9 spinal level. At 1, 2–3, and 4 weeks after injury, the animals underwent urodynamic investigations. Urodynamic investigations showed detrusor overactivity and detrusor-sphincter-dyssynergia appearing over time at 3–4 weeks after injury. Lower urinary tract dysfunction was accompanied by an increase in density of C-fiber afferents in the lumbosacral dorsal horn. CRF-positive Barrington's and 5-HT-positive bulbospinal projections drastically decreased after injury, with partial compensation for the CRF fibers at 3–4 weeks. Interestingly, a decrease over time was observed in the number of GABAergic neurons in the lumbosacral dorsal horn and lamina X, and a decrease of glutamatergic cells in the dorsal horn. Detrusor overactivity and detrusor-sphincter-dyssynergia might therefore arise from a discrepancy in inhibitory/excitatory interneuron activity in the lumbosacral cord as well as input changes which develop over time after injury. The processes point to spinal plastic changes leading to malfunction of the important physiological pathway of lower urinary tract control.

1. Introduction

In an intact organism the bladder distends during filling with an inactive bladder wall (i.e. detrusor) and, simultaneously, the external urethral sphincter (EUS) contracts in order to prevent the leakage of urine. Conversely, during voiding the detrusor contracts and the EUS relaxes (de Groat and Yoshimura, 2015). Initiation of micturition is voluntarily controlled. Although voiding appears like a simple turn on and off action, it is achieved by a complex interaction of the somatic and autonomic nervous system (de Groat et al., 2015). Imaging studies in humans, and electrophysiological and viral tracing studies in animals have shown that the neuronal circuitry controlling lower urinary tract function involves the peripheral nervous system, spinal cord nuclei, brainstem structures, as well as multiple forebrain regions (Karnup and de Groat, 2020; Marson, 1997; Nadelhaft and Vera, 2001).

An insult to the spinal cord that destroys large parts of the white matter will result in neurogenic lower urinary tract dysfunction (Schöps et al., 2015). A well-defined time course of the symptoms has been described in humans, as well as in animal models. Acutely after spinal cord injury, an acontractile/hypocontractile detrusor may lead to urinary retention. Over time, bladder contractions reappear, but voiding is generally inefficient due to the aberrant simultaneous contraction of the EUS (de Groat and Yoshimura, 2006; Panicker et al., 2015; Schneider et al., 2019). This detrusor-sphincter-dyssynergia (DSD) can result in extremely high intravesical pressures that can lead to vesicoureteral reflux and subsequent renal damage (Weld et al., 2000). Additionally to voiding-related troubles, SCI patients experience the emergence of detrusor overactivity, i.e. strong involuntary detrusor contractions that can lead to incontinence episodes and thus have a great impact on patient's quality of life (Simpson et al., 2012).

* Corresponding author at: Institute for Regenerative Medicine, University of Zürich, Wagistrasse 12, 8952 Schlieren, Switzerland.
E-mail address: asartori@bidmc.harvard.edu (A.M. Sartori).
[1] Current address: Department of Medicine, Harvard Medical School, Beth Israel Deaconess Medical Center, Boston, USA.
[2] These authors share the senior authorship.

https://doi.org/10.1016/j.expneurol.2021.113937
Received 29 August 2021; Received in revised form 2 November 2021; Accepted 19 November 2021
Available online 24 November 2021

The anatomical changes that underly lower urinary tract dysfunction are only partially understood. Detrusor overactivity appears to be driven by the sprouting of C-fiber afferents in the lumbosacral cord after SCI (Zinck and Downie, 2008; Zinck et al., 2007). Although these afferents do not convey information about bladder fullness in the healthy system, after SCI they start to fire in response to bladder distension, causing further excitation to the parasympathetic pathway responsible for detrusor contraction (Cheng and de Groat, 2004; Cheng et al., 1999). A lack of inhibition of EUS-motoneurons is hypothesized to be the cause of DSD. A decrease of intraspinal mRNA levels of glutamic acid decarboxylase (GAD) 67 as well as glycine has also been observed (Miyazato et al., 2008; Miyazato et al., 2005).

In this study we assessed the time course of bladder function by urodynamic measurements in spinal cord injured rats, analogous to the corresponding assessments in humans. Results are correlated with anatomical changes in the lumbosacral spinal cord.

2. Materials and methods

2.1. Animals

A total of 20 adult female Lewis rats were investigated in this study [LEW/OrlRj (Lewis); weight, 220–240 g; age, 12–15 weeks old; purchased from Janvier, France]. The rats were initially housed in groups of 4 per cage, and 'single-housed in pairs' (with a separating cage wall) after catheter implantation. Food and water were provided ad libitum. Rats were maintained on a 12:12 h light:dark cycle (light on from 6:30 A.M. until 6:30 P.M). Animals were allocated to one out of four groups, namely: intact ($n = 4$), 1 week after SCI ($n = 5$), 2–3 weeks after SCI ($n = 5$), and 4 weeks after SCI ($n = 6$). All experimental procedures were conducted in accordance with ethical guidelines and were approved by the Veterinary Office of the Canton of Zürich, Switzerland. Behavioral testing and daily stimulation took place in the light phase.

2.2. Bladder catheter and EUS-electrodes implantation

Procedures and surgeries were performed as previously described (Foditsch et al., 2018; Schneider et al., 2015). Briefly, animals were acclimatized to the urodynamic setup for a week before starting with the experiments. Animals were initially anesthetized in 5% Isoflurane (Piramal Healthcare, Digwal, Telangana, India) in air and anesthesia was maintained with an intramuscular injection of Medetomidine (Dormitor, 0.105 mg/kg body weight, Provet AG), Midazolam (Dormicum, 1.4 mg/kg bodyweight, Roche) and Fentanyl (0.007 mg/kg body weight, Kantonsapotheke Zürich). After exposing the bladder, a PE-50 catheter was inserted through the bladder dome and secured in place with a purse-string suture. Two electromyography (EMG) electrodes were placed parallel to urethra, while a ground electrode was secured to the abdominal muscles. Catheter and electrodes were tunneled subcutaneously to the neck of the animals and fixed to a modified infusion harness (QC Single; SAI Infusion Technologies, Lake Villa, IL, USA). Depending on the assigned group, urodynamic and electrophysiological investigations were performed at different time points, namely 14 days after catheter implantation (intact), 1 week after SCI (SCI W1), 2–3 weeks after SCI (SCI W2/3), and 4 weeks after SCI (SCI W4) (Fig. 1). All rats were euthanized by transcardial perfusion in deep anesthesia immediately after the measurements.

2.3. Urodynamic assessment

The catheter was connected to a syringe pump with an in-line pressure transducer, and the electrodes were connected to an amplifier/converter. Saline at room temperature was continuously instilled into the bladder at a constant rate of 120 μl/min over a total duration of 2 h. Pressure, urine volume, voiding, and voltage were recorded simultaneously. The following urodynamic parameters were assessed: Threshold pressure (defined as the detrusor pressure immediately before voiding), maximum detrusor pressure, maximum detrusor pressure during storage phase (defined as the maximum detrusor pressure recorded during the storage phase, i.e. outside of the voiding phase), maximum flow rate, voided volume, voiding time, post-void residual, voiding efficiency, non-voiding contractions, and EUS-EMG (Fig. 2A–I). Maximum detrusor pressure during storage is not described one week after SCI because it is impossible to properly distinguish the storage phase. The animals mainly suffer from overflow incontinence, and the values recorded have been used to describe the voiding phase. Non-voiding contractions were defined as any increase in detrusor pressure bigger than 6 cm H_2O that were not followed by urine flow (Fig. 3, black arrows). Post-void residual was measured immediately after the last voiding by disconnecting the animals from the urodynamic setup and manually emptying the volume present in the bladder on the analytical scale. The EUS-EMG was bandpass-filtered (2–2 kHz). The 45-s-long EMG signal was sliced into 4096 samples, of which 3596 were overlapping (shift is 500 samples). After taking a Hanning window of the signal, a fast Fourier transformation was generated. Quantification of high-frequency EUS-EMG activity was achieved by summing every high-frequency power value in the period of interest, i.e. 4 s before, during (yellow rectangle in Fig. 4A–C), and 4 s after micturition, and dividing it by the sum of every high-frequency power value in the whole period analysed. Data are presented as percentage (Fig. 4D).

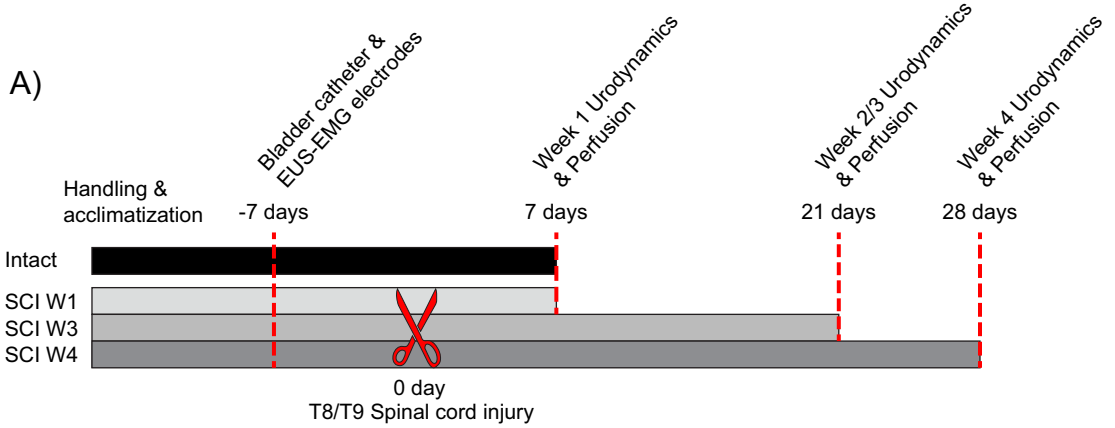

Fig. 1. Study design. All animas were implanted with a bladder catheter and EUS-EMG electrodes on the same day, followed by an incomplete spinal cord injury (red scissors) 7 days later for the animals in the groups SCI W1, SCI W2/3, and SCI W4. (For interpretation of the references to colour in this figure legend, the reader is referred to the web version of this article).

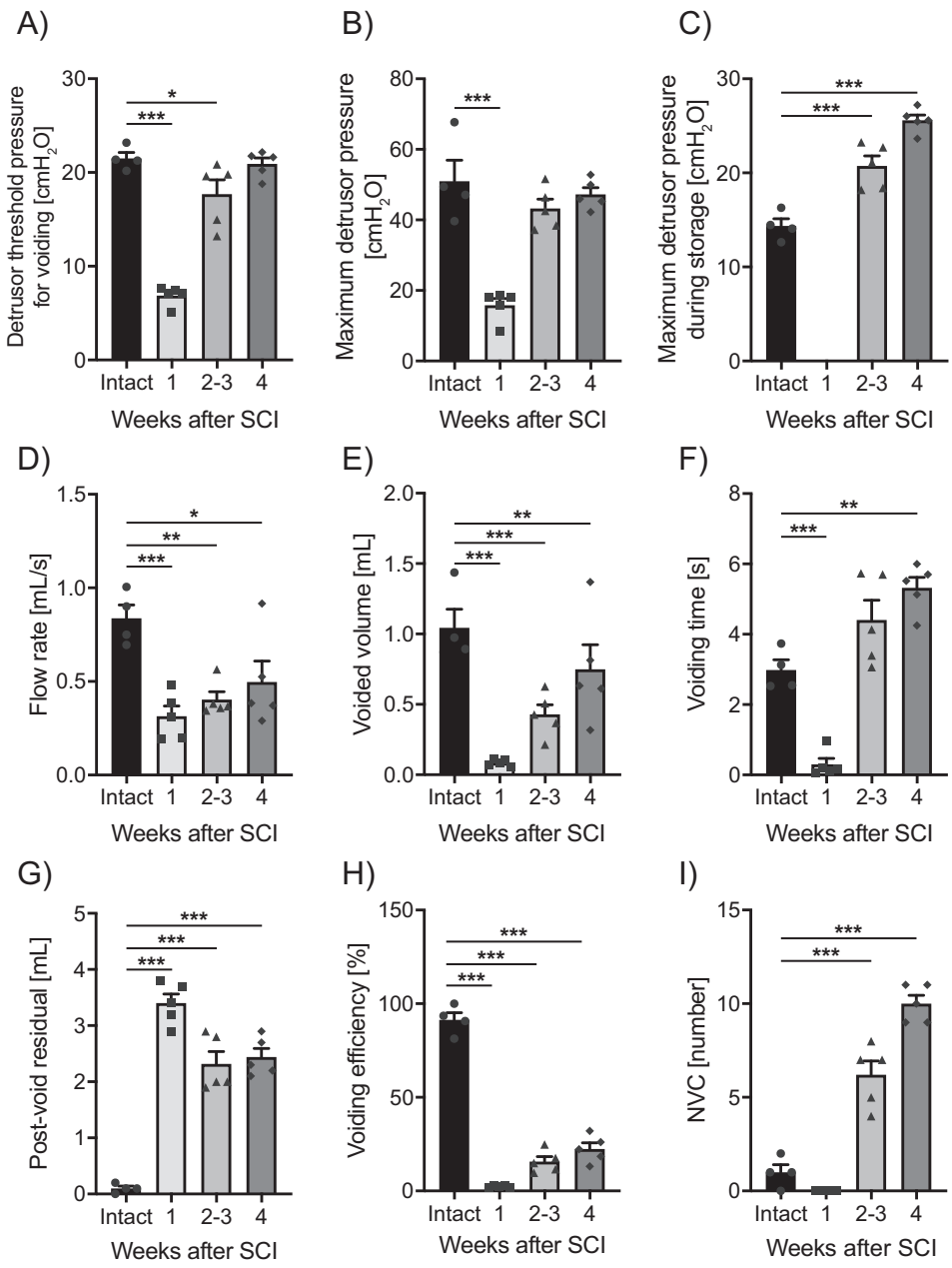

Fig. 2. Comparison of urodynamic parameters before as well as after spinal cord injury. A) Detrusor pressure necessary to trigger micturition (threshold pressure). B) Maximum detrusor pressure. C) Maximum detrusor pressure during storage. D) Maximum flow rate. E) Voided volume. F) Voiding time. G) Post-void residual. H) Voiding efficiency. I) Non-voiding contractions (NVC). Data are shown as means ± standard error of the mean (SEM). $n = 4$ in intact animals and 5 for each of the SCI groups; symbols represent individual animals. *p < 0.05; **p < 0.01; ***p < 0.001.

2.4. Spinal cord injury

One week after bladder catheter and EMG-electrodes implantation, the spinal cord of the animals was incompletely lesioned at the thoracic level 8/9. Surgical procedures were performed as previously described (Schneider et al., 2019). Briefly, animals were initially anesthetized in 5% Isoflurane in air and maintained with an intramuscular injection of Medetomidine, Midazolam and Fentanyl. A T8 laminectomy was performed and the dura was carefully removed. Following the removal of the dura, ca. 90% of the total spinal cord was transected from the dorsal side with iridectomy scissors. The skin was sutured, and the animals let to recover on a heat blanker for 45 min. Analgesics (Rimadyl, 2.5 mg/kg body weight, Pfizer) and antibiotics (Bactrim, 15 mg/kg body weight, Roche) were applied immediately after surgery and daily during the first 14 postoperative days. Afterwards, antibiotics to prevent bladder infections were applied once every second day until the end of the experiment. After injury, the bladders of the animals were manually emptied twice a day for the whole duration of the experiment. One animal in the 4 weeks after SCI group were euthanised the day after SCI due to the weakness caused by an important loss of blood during the surgery.

2.5. Perfusion and tissue preparation

At the end of the study, rats were euthanized with an intraperitoneal overdose of pentobarbital (300 mg/mL, Streuli Pharma, Switzerland). All animals were transcardially perfused with 100 mL Ringer solution containing 1% Heparin (B.Brown Medical Inc., Switzerland), followed by 350 mL of 4% paraformaldehyde (PFA, Sigma-Aldrich, Switzerland) in phosphate buffer (0.1 M, pH 7.4) containing 5% sucrose. Perfusion fixed spinal cords were dissected and post-fixed for 24 h at 4 °C in 4% paraformaldehyde. Afterwards, spinal cords were transferred to a solution of 30% sucrose in 0.1 M phosphate buffer, pH 7.2, and stored for 3 days for cryoprotection. The lumbosacral cords were embedded in

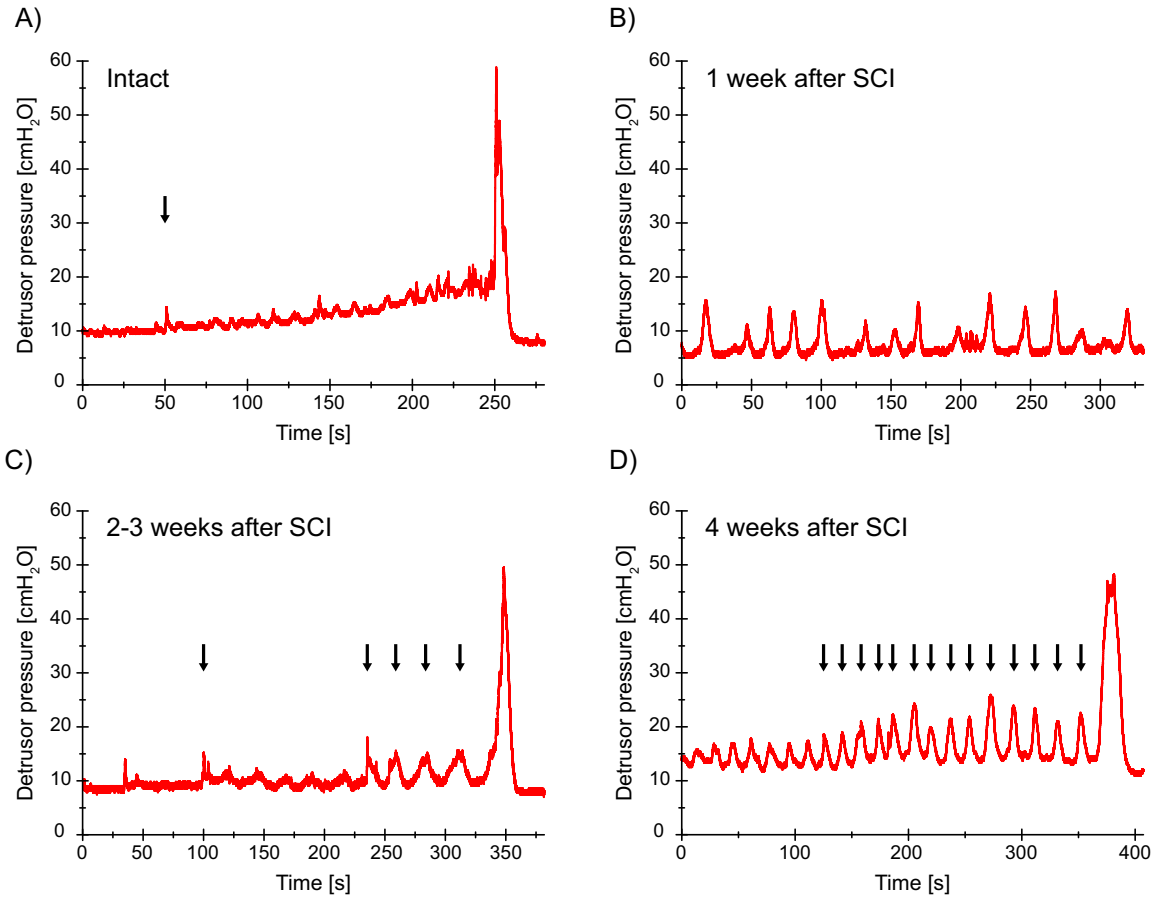

Fig. 3. Detrusor pressure traces of representative, full micturition cycles of: A) intact animals, B) 1 week after SCI, C) 2–3 weeks, and D) 4 weeks after SCI. Black arrows indicate non-voiding contractions. Increases in detrusor pressure shown in panel B are not defined as non-voiding contractions because the animals show overflow incontinence, i.e. no proper voiding cycles are present.

Tissue-Tek OCT compound, frozen in 2-methylbutane (Sigma-Aldrich, Switzerland) cooled to −40 °C with liquid nitrogen, and stored at −20 °C until further processing. L6-S1 spinal cord cross sections were cut on a cryostat either at 40 μm for immunohistological analysis or at 10 μm for in-situ hybridization. Sections used for lesion size assessment were collected on slides (HuberLab, Superfrost), while the remaining sections were collected free-floating in 0.1 M phosphate buffer. For each animal, six to eight of the 10 μm-thick sections of the lumbosacral spinal cord were mounted on a slide, air dried, and then stored at −20 °C until further processing.

2.6. Assessment of lesion completeness

40 μm-thick coronal sections were thawed and rinsed in 0.1 M phosphate buffer. Sections were put on a heating plate at 60 °C for 10 min and then rinsed with water. Afterwards, slides were placed in increasing concentrations of ethanol (70%, 80%, 90%, 80%, 70%) for 30 s each before being rinsed with water and incubated in cresyl violet ($C_{18}H_{15}N_3O_3$, Sigma-Aldrich, Switzerland). After 5 min, sections were placed in increasing concentrations of ethanol (70%, 80%, 90%, 95%, 100%, 100%) for 30 s each, followed by a final wash in Xylene (90 s), before being coverslipped with Eukitt. Cresyl violet images were used to manually reconstruct the maximal lesion extent in a spinal cord template based on a spinal cord atlas (*The spinal cord – A Christopher and Dana Reeve Foundation Test and Atlas, 2009*) using Adobe Illustrator CC 2020. The percentage of spared white matter area was determined using ImageJ/Fiji (Schindelin et al., 2012).

2.7. Immunofluorescence

Free-floating sections were blocked and permeabilized in TNB blocking solution containing 0.3% Triton-X and 5% normal goat serum for 60 min at room temperature, before being incubated with the primary antibody (rabbit-anti-CGRP, 1:750, Cat. Nr. AB15360, Millipore, Burlington, MA, USA; rabbit-anti-5HT, 1:2000, Cat. Nr. 20,080, ImmunoStar, Hudson, WI, USA; rabbit-anti-CRF, 1:400, Cat. Nr. #PBL rC68, Salk Institute for Biological Studies, San Diego, CA, USA) diluted in TNB containing 0.05% Triton-X overnight at 4 °C. The sections were then washed three time in 0.1 M PBS for 10 min each, incubated with secondary antibody (goat-anti-rabbit conjugated to Alexa Fluor 647; 1:500, Cat. Nr. 111-605-144, Jackson ImmunoResearch Laboratories, West Grove, PA, USA) for 2 h at room temperature, counterstained with 4′,6-Diamidino-2-Phenylindole (DAPI, 1:1000, Cat. Nr. 268,298, Sigma-Aldrich, St. Louis, MO, USA), and ultimately washed three times in 0.1 M PBS and once in 0.05 M Tris for 10 min each. Sections were mounted on slides, air-dried overnight at 4 °C, and coverslipped with fluorescence mounting medium (Mowiol, Merck).

2.8. In-situ hybridization (RNAscope)

Sequences of targets, preamplifiers, amplifiers, and label probes are proprietary and commercially available (Advance Cell Diagnostics). In this study, we used probes against rat choline acetyltransferase (ChAT-C1), vesicular glutamate transporter 2 ($vGluT_2$, Slc17a6-C3), glycine transporter 2 ($GlyT_2$, Slc6a5-C1), glutamic acid decarboxylase 2 (GAD_2-C2), and cFos (c-Fos-C4). Experimental protocols were

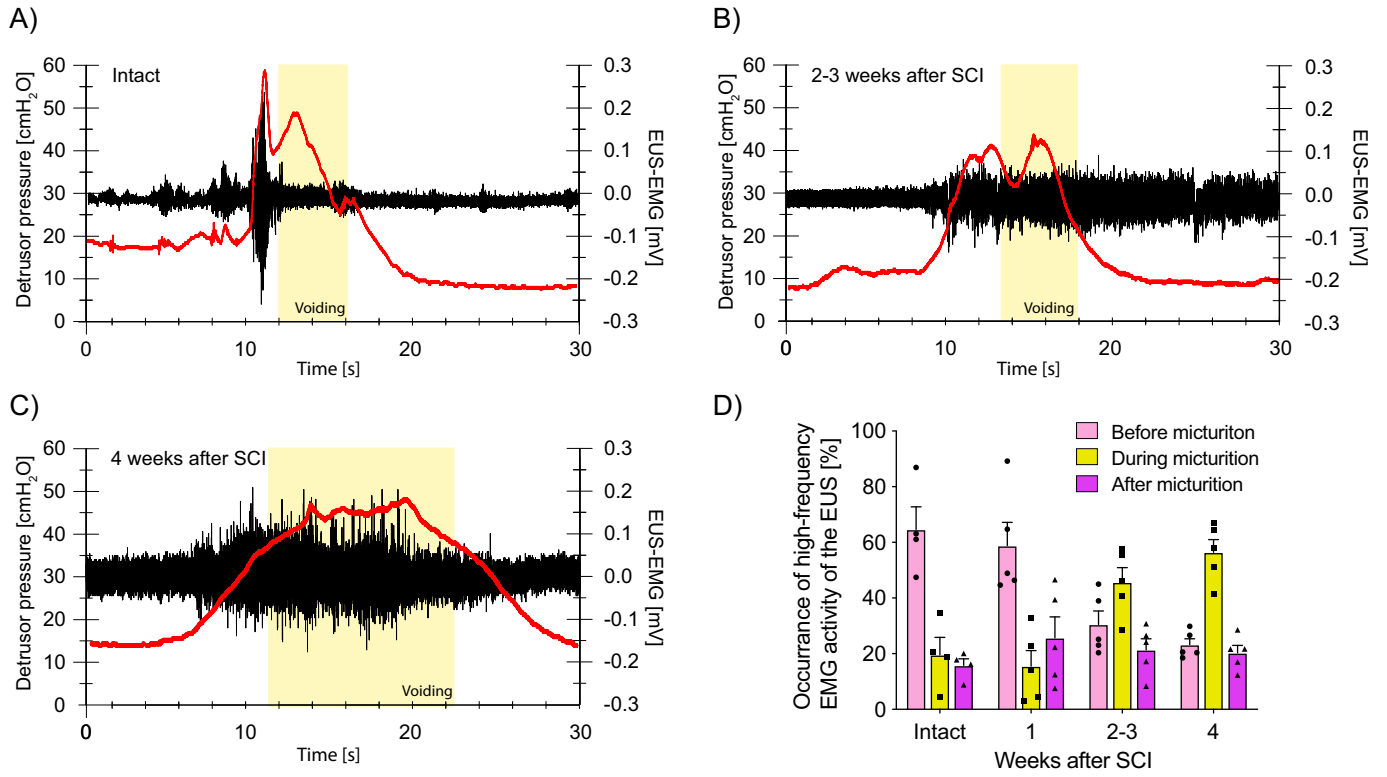

Fig. 4. Representative traces of the EMG activity of the external urethral sphincter (EUS; black) and the detrusor pressure (red line) in A) intact animals, or spinal cord injured rats B) 2–3 weeks and C) 4 weeks after SCI. The yellow rectangle indicates the voiding phase. D) Quantification of occurrence of high-frequency EMG activity of the EUS before (pink), during (yellow), and after (violet) micturition for the four investigated groups. (For interpretation of the references to colour in this figure legend, the reader is referred to the web version of this article).

conducted according to manufacturer's instructions and have been previously described(Schneider et al., 2019). Briefly, endogenous peroxidases were quenched with hydrogen peroxide (Advanced Cell Diagnostics) for 10 min at room temperature. Sections were placed in antigen retrieval buffer (Advanced Cell Diagnostics) for 10 min at 98–100 °C, before application of the protease treatment (Protease Plus, Advanced Cell Diagnostics) for 30 min at 40 °C. Sections were then incubated with a mix containing the hybridization probes either for ChAT, vGluT2, and c-Fos or GlyT2, GAD2, and c-Fos for 2 h at 40 °C. The hybridization probes were then amplified and developed using the Tyramide Signal Amplification (TSA) Plus Fluorescein, TSA Plus Cyanine 3, and TSA Plus Cyanine 5 (TSA Plus Fluorescence Palette, NEL760001KT, PerkinElmer) and counterstained with DAPI (Advanced Cell Diagnostics). Slides were coverslipped using fluorescence mounting medium (Mowiol, Merck).

3. Quantification of immunofluorescent signal

Three cross-sections of the spinal levels L6-S1 were randomly picked and imaged with either a confocal (20×, Leica, inverted Leica SP8) or a fluorescent microscope (20×; Zeiss, Axio Scan.Z1). Exposure time and laser-related parameters were optimized during the first imaging and kept constant across all sections. Maximum intensity projections were created, and pictures were exported in TIFF format for investigation. Further analyses were performed with ImageJ/Fiji (open source software, ImageJ.net). The mean gray values for the regions of the lamina X and the ventral horn (5-HT), lamina X and intermedio-lateral column (CRF), and dorsal horn (CGRP) were measured for the three sections and averaged after subtracting the background value. The values were normalized to the corresponding values of the intact group.

3.1. Quantification of in-situ hybridization

Three cross-sections of each spinal level L6-S1 were randomly picked and imaged with a fluorescent microscope (20×; Zeiss, Axio Scan.Z1). Mosaic pictures were acquired and merged with the Zeiss software. Maximum intensity projections were created, and pictures were exported in TIFF format for analysis. Pictures were imported in Adobe Illustrator CC2020 and labelled neurons were manually marked. The coordinates of each marked neuron were retrieved with ImageJ/Fiji, and then used to plot the cells to a standardized spinal cord cross-section template (*The spinal cord – A Christopher and Dana Reeve Foundation Test and Atlas, 2009)* with Matlab (The MathWorks, 2018b). The numbers of ChAT-positive, GlyT2-positive, GAD2-positive, and vGluT2-positive cells were calculated within the laminae 1, 2, and 3, which reflect the dorsal horn; laminae 4 and 5, which comprehend the intermedio-lateral column; and lamina X. Additionally, cells positive for the before mentioned markers as well as for the immediate early gene c-Fos were marked and counted separately.

3.2. Statistical analysis

During the whole duration of the experiments, animals were randomly number-coded, and investigators were blinded until the end of the analysis. Data are reported as means ± standard error of the mean (SEM). A one-way ANOVA followed by Bonferroni's post-hoc testing was used to investigate the differences in the urodynamic parameters as well as for the immunofluorescence analysis. To avoid multiple testing as much as possible, the three groups involving SCI animals were not compared between each other but only to the value of the intact group. A two-way ANOVA followed by Bonferroni's post-hoc testing was used to analyze the in-situ hybridization results. The value of significance was considered at $p < 0.05$. Statistical analysis and plotting of data were

performed using Stata statistical software (Version 14, StataCorp) and GraphPad Prism 8 (GraphPad Software).

4. Results

4.1. Urodynamic findings in intact and spinal cord injured rats

We performed urodynamic investigations in adult rats with either an intact or an incompletely injured spinal cord (Fig. 1). The thoracic transections severed between 82 and 94% of the total spinal cord cross section, and the extent of the lesion did not differ between the groups with the different survival times (data not shown). Lower urinary tract function of spinal cord injured animals was assessed at 1 week, 2–3 weeks, or 4 weeks after SCI. Intact animals were analysed 14 days after catheter and electrode implantation. In intact animals, urodynamic tracings with bladder filling showed a gradual increase in intravesical pressure until micturition was triggered (Fig. 2, Fig. 3A). During voiding, EMG activity of the EUS decreased (Fig. 4A), allowing a rapid and efficient release of the urine (Fig. 2).

In the injured groups, one week after SCI, lower urinary tract function was absent as demonstrated by an acontractile detrusor during the urodynamic investigation (Figs. 2, 3B). The voiding reflex began to reappear 2–3 weeks after SCI, but was not sufficient for voiding larger volumes in most of the cases because of the simultaneous contraction of the EUS, a condition typical for DSD (Fig. 2, Fig. 3C, 4B). Four weeks after SCI, lower urinary tract dysfunction was confirmed by the urodynamic investigation (Figs. 2, 3D, 4C). Over time, SCI induced an increased activity of the EUS during micturition (Fig. 4D), which resulted in significant augmentation in maximum intravesical pressure during storage (Fig. 2C), decreased maximum flow rate (Fig. 2D), diminished voided volume (Fig. 2E), increased voiding time (Fig. 2F), bigger post-void residual (Fig. 2G), reduced voiding efficiency (Fig. 2H), and increased number of non-voiding contractions, i.e. detrusor overactivity (Fig. 2I, black arrows in Fig. 3).

4.2. Spinal projections originating from supraspinal nuclei decrease after SCI

We then examined the anatomical changes in the spinal cord associated with and possibly causing neurogenic lower urinary tract dysfunction. First, we quantified two kinds of important supraspinal projections to the lumbosacral cord. In intact animals, a dense serotonergic (5-HT positive) innervation was observed in lamina X as well as in the ventral horn (Fig. 5A). Acutely after SCI, the density of 5-HT-positive fibers dropped to less than half in both lamina X and ventral horn (Fig. 5B—D). 5-HT fiber density slightly increased over time, but remained severely affected up to 4 weeks after SCI (Fig. 5C—D). We also analysed the bulbospinal corticotropin-releasing factor (CRF)-positive projections to the lower spinal cord originating from the pontine micturition center (PMC or Barrington's nucleus) that are specifically involved in lower urinary tract function (Valentino et al., 1994; Verstegen et al., 2017).xTwo main regions receive a high density of CRF-positive fibers in intact rats, namely the intermedio-lateral column with the preganglionic autonomic neurons (IML) and lamina X (Fig. 6A–F). The density of CRF-positive fibers drastically decreased after SCI (Fig. 6C, F), but, interestingly, recovered to a certain extent over the course of 4 weeks. Nonetheless, at 4 weeks after SCI the CRF-positive innervation in the IML and lamina X remained significantly decreased by about 70% and 50%, respectively, compared to the density present in intact animals (Fig. 6C, F).

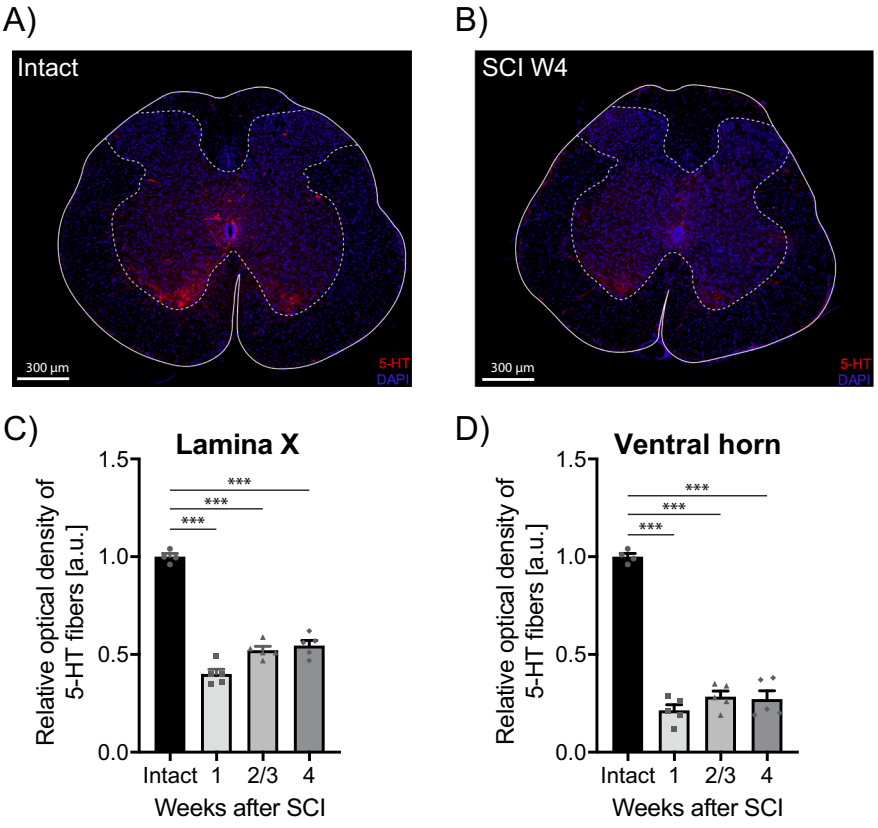

Fig. 5. Serotonergic innervation in the lumbosacral cord. Representative images of 5-HT positive fibers in A) intact and B) spinal cord injured rats 4 weeks after lesion. Sections were counterstained with DAPI. C—D) Relative optical density quantification for 5-HT signal in the C) lamina X and D) ventral horn in intact and 1, 2–3, and 4 weeks after injury. ***$p < 0.001$.

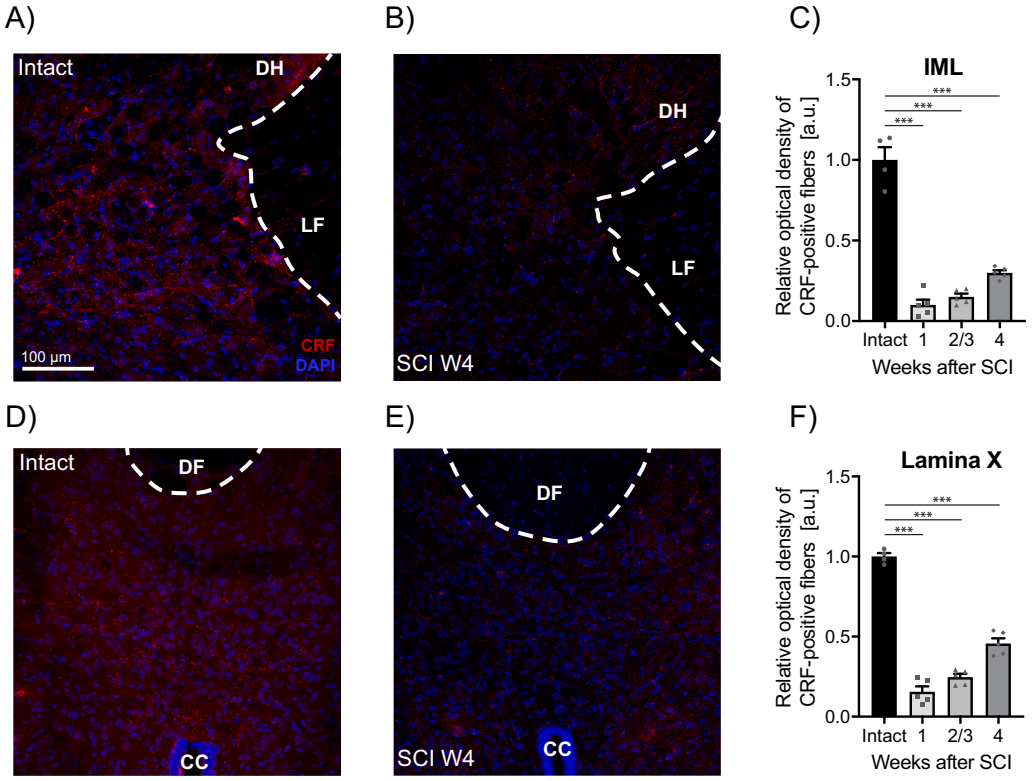

Fig. 6. Innervation of the lumbosacral spinal cord by CRF-positive Barrington's nucleus fibers. A, B, D, E) Immunofluorescent CRF-positive fibers and terminals are concentrated in the intermedio-lateral column (IML) and lamina X. Sections were counterstained with DAPI. C, F) Relative optical density quantification for CRF in the C) IML and F) lamina X. CC = central canal; DF = dorsal funinculus; DH = dorsal horn; DF = dorsal funinculus. ***$p < 0.001$.

4.3. Type-C bladder afferent fibers sprout over time after SCI

Using calcitonin gene related peptide (CGRP) as a marker, we labelled primary afferent fibers of type C in the lumbosacral cord (Fig. 7A–B). Typically, CGRP positive fibers were limited to the superficial dorsal horn of intact animals (Fig. 7A). No difference in the CGRP-positive fiber density was observed acutely after SCI. However, starting at 2–3 weeks after SCI the density of CGRP-positive fibers in lamina 1 and 2 gradually increased to reach a level around 50% over the original density at four weeks after SCI (Fig. 7B,C).

4.4. SCI decreases the number of inhibitory and excitatory neurons in the lumbosacral spinal cord

In the 2 h preceding euthanasia at each time point (intact, 1, 2–3 and 4 weeks after SCI), the animals were subjected to continuous cycles of bladder filling and voiding over 2 h in order to strongly stimulate the neurons involved in urinary tract function. We assessed their activation status then by subsequent immunofluorescent labelling for c-Fos followed by markers for cholinergic (ChAT), glutamatergic (vGlut2), glycinergic (GlyT2), and GABAergic (GAD2) neurons. mRNA localization was used to identify all cholinergic, glutamatergic, glycinergic, and GABAergic neurons in the spinal segments L6-S1. We did not observe differences between intact and spinal cord lesioned animals for the total number of glycinergic cells (GLYT2 mRNA-positive) or cholinergic

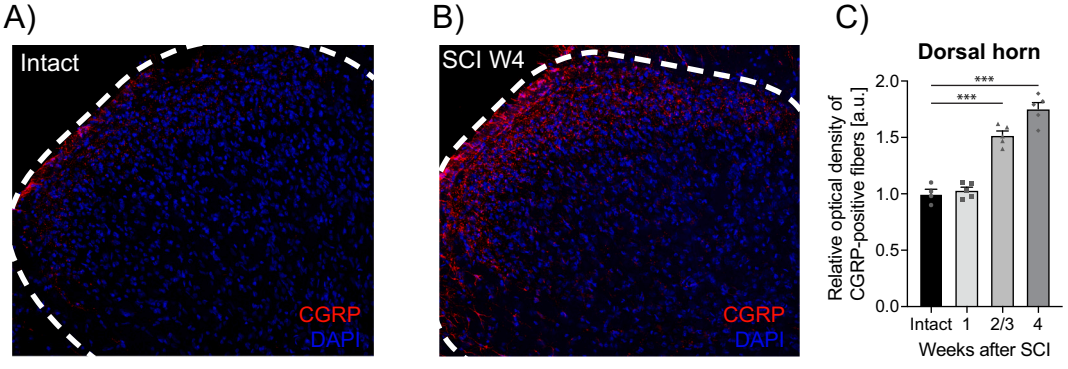

Fig. 7. Assessment of C-fiber afferents in the lumbosacral dorsal horn. A-B) Calcitonin gene-related peptide (CGRP) staining in the superficial dorsal horn (dotted line) of A) intact and B) spinal cord injured rats 4 weeks after lesion. Sections were counterstained with DAPI. C) Mean optical density quantification for CGRP in the dorsal horn. ***$p < 0.001$.

neurons (CHAT mRNA-positive) in any of the regions investigated (Fig. 8A, C, E, G). In contrast, a gradual, significant decrease over time after SCI was observed for the glutamatergic neurons (VGLUT2 mRNA-positive) in the laminae 1, 2, 3 of the dorsal horn, but not in laminae 4–5 and 10 (Fig. 8B, F). Interestingly, the number of GABAergic cells (GAD2 mRNA-positive) decreased after SCI by 20–30% in the laminae 1, 2, 3, as well as in laminae 4, 5 (Fig. 8D, H). The proportions of glutamatergic and GABAergic neurons expressing the activation marker c-Fos after 2 h of continuous micturition cycles were examined in laminae 1–3, 4–5 and 10 (Fig. 8I–J). In the intact animals, about 15% of the total glutamatergic or GABA-ergic interneurons in laminae 1–3 and 10 (6% in laminae 4–5) showed increased levels of c-Fos mRNA in response to repeated micturition (Fig. 8I–J). The numbers of activated neurons were reduced to less than half of these values 1 week after lesion, reflecting the hypoactivity of the circuits acutely after SCI. The reduction of the double labelled glutamatergic cells in the dorsal horn recovered only slightly over time (Fig. 8I) and was in line with the reduction in the number of total glutamatergic cells in this region (Fig. 8F). In contrast, lamina 10 glutamatergic cells activated by micturition recovered to almost the intact level at 4 weeks after injury (Fig. 8I). The number of GABAergic, micturition-activated cells decreased in all laminae analysed. Recovery was only partial, except for laminae 4–5 (Fig. 8J). Only few cholinergic and glycinergic cells were double labelled in each spinal cord cross section (data not shown).

5. Discussion

The storage and periodic release of urine require the coordinated, antagonistic actions of the detrusor and the external urethral sphincter. Rats with large but incomplete spinal cord injuries developed a typical, if untreated (by manual voiding) fatal malfunction characterized mainly by the abnormal, simultaneous contraction of detrusor and EUS. This circuit malfunction developed over time after injury and resembles closely the urodynamic malfunction in spinal cord injured humans. On the level of neuroanatomy, descending reticulospinal projections were severely affected below the injury, resulting in a large decrease of supraspinal inputs to the lumbosacral interneurons and bladder motoneurons. C-type afferents increased their projection to layers 1–2 of the dorsal horn, probably causing an increased stimulation of the parasympathetic pathways leading to detrusor contraction. Surprisingly, two spinal interneuron populations, GABAergic and glutamatergic neurons in the dorsal horn and in lamina X, showed a major loss of cells after SCI, raising the possibility that the lack of inhibitory inputs is a principal cause for DSD and detrusor overactivity.

Similar to human SCI patients and as previously reported (Bywater et al., 2018; de Groat and Yoshimura, 2006; Panicker et al., 2015), after

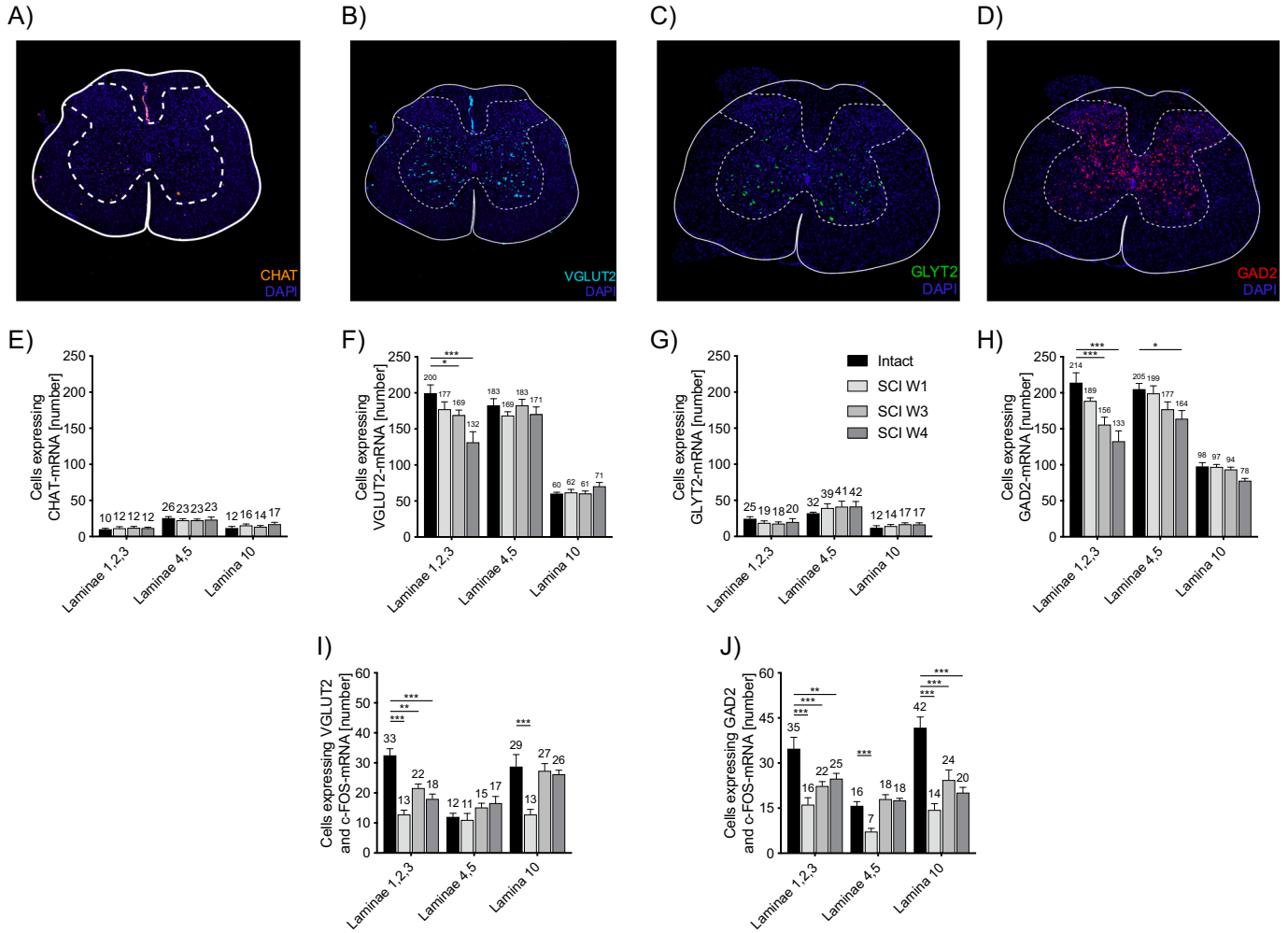

Fig. 8. Cholinergic, glutamatergic, glycinergic, and GABAergic neurons in the sacral cord of intact and spinal cord injured rats 1, 2/3, and 4 weeks after injury. A–D) Representative images of in-situ hybridization for mRNA of A) ChAT, B) vGluT2, C) GlyT2, and D) GAD2. Sections were counterstained with DAPI. E–H) Quantification of E) cholinergic, F) glutamatergic, G) glycinergic, and H) GABAergic neurons in the sacral cord of intact animals as well as spinal cord injured rats 1 week (SCI W1), 2/3 weeks (SCI W2/3), and 4 weeks (SCI W4) after injury. I–J) Quantification of I) glutamatergic and J) GABAergic neurons that simultaneously expressed the c-FOS mRNA induced by 2 h of repeated bladder filling and voiding cycles. *$p < 0.05$; **$p < 0.01$; ***$p < 0.001$.

a lesion to the spinal cord the lower urinary tract of the rat shows a sequence of characteristic functional changes. Initially, there is a phase in which the detrusor is acontractile, resulting in overflow incontinence and high post-void residuals. Starting at 2–3 weeks after injury, urodynamic investigations showed an abnormal increase of high frequency EUS-EMG signals during voiding, a hallmark of DSD. EUS contraction during voiding resulted in an interrupted stream of urine, demonstrated by a longer voiding time and a reduced maximum flow rate, and high intravesical pressures that remain elevated for a prolonged period due to the increased outlet resistance. Interestingly, a major difference is present between the human and rodent lower urinary tract dysfunction. In fact, chronic spinal cord injured patients suffering from DSD will show higher intravesical pressures during voiding compared to non-lesioned subjects (Panicker et al., 2015): While this difference was not present in our animals, the prolonged period of high intravesical pressure may also increase the chance for urinary reflux to the kidneys.

In this study, we did not compare SCI groups between each other, since it is extremely difficult to compare early versus late stages of neurogenic lower urinary tract dysfunction. In fact, acutely after injury the animals mainly exhibit overflow incontinence during urodynamic investigations, which is an entirely different behavior compared to the more chronic stages.

We have observed a significant increase in primary afferent C-fiber density in the superficial layers of the dorsal horn 4 weeks after SCI. Fiber numbers increased, but the C-fibers remained in their appropriate layers 1 and 2. Sprouting of C-type afferents is discussed as an important candidate mechanism for the development of detrusor overactivity. In healthy conditions, these afferents do not convey information about bladder fullness to the central nervous system (Häbler et al., 1990). However, in chronic SCI the C-fibers respond to bladder distension, possibly causing an hyperexcitation of the parasympathetic pathway and thus triggering detrusor overactivity (de Groat et al., 1990). Nonetheless, the etiology of detrusor overactivity is not completed resolved, and its emergence might not be entirely due to processes taking place in the central nervous system. Detrusor overactivity and DSD follow similar time-courses, raising the important question if DSD, which causes an obstruction, might be at the basis of detrusor overactivity. In fact, animal models of bladder outlet obstruction (BOO) have been frequently used to investigate detrusor overactivity, since surgical obstruction is enough to drive the emergence of the symptoms over time (Brading, 1997; Park et al., 2018). Proteomic analysis of the urothelium of rats subjected to BOO pointed towards the importance and correlation of detrusor overactivity with an inflammatory response (Park et al., 2018). Similarly, amount of neurotrophic factors such as nerve growth factor (NGF) and brain-derived neurotrophic factor (BDNF) present in the bladder wall have been described to be correlated with the severity of detrusor overactivity (Coelho et al., 2019; Ha et al., 2011), further elucidating the challenges in understating the exact mechanisms underlying overactive bladder.

Several supraspinal nuclei are involved in the proper functioning of the lower urinary tract in a healthy system. These mainly include the pontine micturition center/Barrington's nucleus, the periaqueductal gray, the hypothalamus, and the motor cortex (Andersson and Arner, 2004; Nadelhaft and Vera, 2001; Verstegen et al., 2019; Yao et al., 2019). The descending reticulospinal projections were severely affected by the SCI, resulting in a large decrease of spinal coverage below the level of the lesion including the CRF-positive fibers originating in the pontine micturition center, the main nucleus responsible for voiding initiation, as well as 5-HT-positive fibers from the raphe system (Ahn et al., 2018). 5-HT fibers regulate the level of excitation in different spinal circuits; they facilitate the urinary guarding reflex by inhibiting the parasympathetic pathway that causes detrusor contraction (Chang et al., 2007; Khaled and Elhilali, 2003). Administration of 5-HT1a receptor agonists has been shown to improve symptoms of DSD and detrusor overactivity in spinal cord injured rats (Lin et al., 2020), clearly demonstrating the importance of this projection system for the correct functioning of the lower urinary tract. 5-HT fiber density remained low, without detectable compensatory sprouting, also 4 weeks after injury. Together with estrogen receptor 1 alpha (ESR1)-positive pontine neurons, the CRF-positive neurons are the other main cell population of the pontine micturition center (Keller et al., 2018; Valentino et al., 1994; Verstegen et al., 2017). The CRF-positive innervation of the lumbosacral cord decreased to less than 10% 1 week after injury (Studeny and Vizzard, 2005). Contrarily to the serotonergic innervation, over the subsequent 3 weeks a partial restoration of CRF fiber density, probably due to local, short-range sprouting of spared descending fibers, was observed. This sprouting reestablished in the intermedio-lateral column about 30% and in lamina X to about 46% of the initial fiber density. Since neurons in the PMC are exclusively glutamatergic (Verstegen et al., 2017), they have to synapse onto downstream inhibitory interneurons in order to induce the relaxation of the EUS during normal voiding. In fact, PMC projections are known to synapse onto GABAergic and glycinergic neurons in the lumbosacral cord (Blok and Holstege, 2000; Sie et al., 2001), and we previously showed a decrease in the overall number of neurons positive for GAD2-mRNA in the lamina X of the lumbosacral spinal cord four weeks after SCI. In the present study, we showed a gradual reduction over time in the number of excitatory (vGluT2-mRNA positive) and inhibitory (GAD2-mRNA positive) neurons in the dorsal horn (Laminae I-III) as well as Laminae IV-V (GAD2-mRNA only). Simultaneous labelling of lower urinary tract-related active cells with cFos-mRNA confirmed the reduction over time of these cells in the dorsal horn but, interestingly, not of the GAD2-mRNA positive neurons in Lamina IV-V, indicating that these cells are involved in other neuronal circuits. Importantly, we observed a reduction in the number of lower urinary tract-related active (cFos-positive) GABAergic neurons in Lamina X, which was not detected, at least in a significant manner, in the total number of GABAergic cells.

Our findings of a decreased number of GABAergic interneurons in the relevant spinal layers and of GABA/c-Fos interneurons during bladder filling/voiding cycles fits well with the mechanistic hypothesis that a lack of inhibitory signals in the lumbosacral cord is a crucial reason for the major lower urinary tract dysfunction after spinal cord injury, i.e. DSD and detrusor overactivity and that these arise over time with the reduction of inhibitory inputs at the level of the lumbosacral spinal cord. Supporting this, a decrease in intraspinal GAD mRNA as well as glycine has also been reported after SCI (Miyazato et al., 2008; Miyazato et al., 2003). In addition, we showed that acutely after injury, i.e. one week after SCI, these neurons are still present but not active during filling-induced voiding behavior, thus supporting the idea that the initial phase of urinary retention and bladder acontractility is mainly due to the spinal shock phase.

Overall, detrusor overactivity and DSD are not present acutely after the spinal cord lesion, but rather develop over time, in the present rat model as well as in human patients (Groen et al., 2016; Panicker et al., 2015; Samson and Cardenas, 2007). The time course investigated in the present study suggests that, together with the rearrangement of supraspinal inputs to the lumbosacral spinal cord, local sprouting of sensory and descending motor fibers, and plastic rearrangements could be a crucial factor for the emergence of urinary symptoms. Local interneurons could not be activated by experimental filling and voiding of the bladder acutely after injury, reflecting the spinal cord shock phase. At 4 weeks after injury, GABA and VGTLUT2-containing interneurons showed a reduction in number, in particular the lower urinary tract-related neurons of laminae I-III as well as lamina X.

6. Conclusions

In conclusion, similarly to humans, neurogenic lower urinary tract dysfunction after SCI in rats is characterized by different phases: an acontractile/hypocontractile detrusor and related lumbosacral interneurons acutely after spinal cord injury, followed by the development of an aberrant, simultaneous contraction of the detrusor and the external

urethral sphincter in the more chronic phase. Detrusor overactivity is possibly influenced by the sprouting of afferent fibers of type C in the dorsal horn responding to bladder distension, while detrusor-sphincter-dyssynergia might be driven by decreased bulbospinal input to and a reduced number of inhibitory GABAergic interneurons in the lumbosacral cord.

Authors contributions

AMS, TMK, and MES initiated, conceived, and designed the study. AMS conducted the experiments with the help of ASH, MIS, and RR. AMS, TMK, and MES performed data analysis. AMS designed the figures and wrote the initial draft of the manuscript. All authors critically revised the manuscript and approved its final version.

Authors disclosure statement

The authors have no conflict of interest to declare.

Funding statement

This project was funded by grants of the Spinal Cord Consortium of the Christopher and Dana Reeve Foundation, the Santa Casa da Misericòrdia de Lisboa (Prémio Mello e Castro- 2016), and by the UZH Foundation (University of Zürich).

Acknowledgements

We would like to thank Martin Wieckhorst, Hansjörg Kasper, and Stefan Giger (University of Zürich) for their great support in technical matters. Imaging was performed with support of the Center for Microscopy and Image Analysis of the University of Zürich.

References

Ahn, J., Saltos, T.M., Tom, V.J., Hou, S., 2018. Transsynaptic tracing to dissect supraspinal serotonergic input regulating the bladder reflex in rats. Neurourol. Urodyn. 37, 2487–2494.
Andersson, K.E., Arner, A., 2004. Urinary bladder contraction and relaxation: physiology and pathophysiology. Physiol. Rev. 84, 935–986.
Blok, B.F., Holstege, G., 2000. The pontine micturition center in rat receives direct lumbosacral input. An ultrastructural study. Neurosci. Lett. 282, 29–32.
Brading, A.F., 1997. A myogenic basis for the overactive bladder. Urology 50, 57–67 (discussion 68-73).
Bywater, M., Tornic, J., Mehnert, U., Kessler, T.M., 2018. Detrusor acontractility after acute spinal cord injury-myth or reality? J. Urol. 199, 1565–1570.
Chang, H.Y., Cheng, C.L., Chen, J.J., de Groat, W.C., 2007. Serotonergic drugs and spinal cord transections indicate that different spinal circuits are involved in external urethral sphincter activity in rats. Am. J. Physiol. Ren. Physiol. 292, F1044–F1053.
Cheng, C.L., de Groat, W.C., 2004. The role of capsaicin-sensitive afferent fibers in the lower urinary tract dysfunction induced by chronic spinal cord injury in rats. Exp. Neurol. 187, 445–454.
Cheng, C.L., Liu, J.C., Chang, S.Y., Ma, C.P., de Groat, W.C., 1999. Effect of capsaicin on the micturition reflex in normal and chronic spinal cord-injured cats. Am. J. Phys. 277, R786–R794.
Coelho, A., Oliveira, R., Antunes-Lopes, T., Cruz, C.D., 2019. Partners in crime: NGF and BDNF in visceral dysfunction. Curr. Neuropharmacol. 17, 1021–1038.
de Groat, W.C., Yoshimura, N., 2006. Mechanisms underlying the recovery of lower urinary tract function following spinal cord injury. Prog. Brain Res. 152, 59–84.
de Groat, W.C., Yoshimura, N., 2015. Anatomy and physiology of the lower urinary tract. Handb. Clin. Neurol. 130, 61–108.
de Groat, W.C., Kawatani, M., Hisamitsu, T., Cheng, C.L., Ma, C.P., Thor, K., Steers, W., Roppolo, J.R., 1990. Mechanisms underlying the recovery of urinary bladder function following spinal cord injury. J. Auton. Nerv. Syst. 30 (Suppl), S71–S77.
de Groat, W.C., Griffiths, D., Yoshimura, N., 2015. Neural control of the lower urinary tract. Compr. Physiol. 5, 327–396.
Foditsch, E.E., Roider, K., Sartori, A.M., Kessler, T.M., Kayastha, S.R., Aigner, L., Schneider, M.P., 2018. Cystometric and external urethral sphincter measurements in awake rats with implanted catheter and electrodes allowing for repeated measurements. J. Vis. Exp. 131, e56506. https://doi.org/10.3791/56506.
Groen, J., Pannek, J., Castro Diaz, D., Del Popolo, G., Gross, T., Hamid, R., Karsenty, G., Kessler, T.M., Schneider, M., t Hoen, L., Blok, B., 2016. Summary of European Association of Urology (EAU) guidelines on neuro-urology. Eur. Urol. 69, 324–333.
Ha, U.S., Park, E.Y., Kim, J.C., 2011. Effect of botulinum toxin on expression of nerve growth factor and transient receptor potential vanilloid 1 in urothelium and detrusor muscle of rats with bladder outlet obstruction-induced detrusor overactivity. Urology 78, 721.e721–721.e726.
Häbler, H.J., Jänig, W., Koltzenburg, M., 1990. Activation of unmyelinated afferent fibres by mechanical stimuli and inflammation of the urinary bladder in the cat. J. Physiol. 425, 545–562.
Karnup, S.V., de Groat, W.C., 2020. Propriospinal neurons of L3-L4 segments involved in control of the rat external urethral sphincter. Neuroscience 425, 12–28.
Keller, J.A., Chen, J., Simpson, S., Wang, E.H., Lilascharoen, V., George, O., Lim, B.K., Stowers, L., 2018. Voluntary urination control by brainstem neurons that relax the urethral sphincter. Nat. Neurosci. 21, 1229–1238.
Khaled, S.M., Elhilali, M., 2003. Role of 5-HT receptors in treatment of overactive bladder. Drugs Today (Barc) 39, 599–607.
Lin, C.Y., Sparks, A., Lee, Y.S., 2020. Improvement of lower urinary tract function by a selective serotonin 5-HT(1A) receptor agonist, NLX-112, after chronic spinal cord injury. Exp. Neurol. 332, 113395.
Marson, L., 1997. Identification of central nervous system neurons that innervate the bladder body, bladder base, or external urethral sphincter of female rats: a transneuronal tracing study using pseudorabies virus. J. Comp. Neurol. 389, 584–602.
Miyazato, M., Sugaya, K., Nishijima, S., Ashitomi, K., Hatano, T., Ogawa, Y., 2003. Inhibitory effect of intrathecal glycine on the micturition reflex in normal and spinal cord injury rats. Exp. Neurol. 183, 232–240.
Miyazato, M., Sugaya, K., Nishijima, S., Ashitomi, K., Morozumi, M., Ogawa, Y., 2005. Dietary glycine inhibits bladder activity in normal rats and rats with spinal cord injury. J. Urol. 173, 314–317.
Miyazato, M., Sasatomi, K., Hiragata, S., Sugaya, K., Chancellor, M.B., de Groat, W.C., Yoshimura, N., 2008. GABA receptor activation in the lumbosacral spinal cord decreases detrusor overactivity in spinal cord injured rats. J. Urol. 179, 1178–1183.
Nadelhaft, I., Vera, P.L., 2001. Separate urinary bladder and external urethral sphincter neurons in the central nervous system of the rat: simultaneous labeling with two immunohistochemically distinguishable pseudorabies viruses. Brain Res. 903, 33–44.
Panicker, J.N., Fowler, C.J., Kessler, T.M., 2015. Lower urinary tract dysfunction in the neurological patient: clinical assessment and management. Lancet Neurol. 14, 720–732.
Park, E.C., Lim, J.S., Kim, S.I., Lee, S.Y., Tak, Y.K., Choi, C.W., Yun, S., Park, J., Lee, M., Chung, H.K., Kim, K.S., Na, Y.G., Shin, J.H., Kim, G.H., 2018. Proteomic analysis of Urothelium of rats with detrusor overactivity induced by bladder outlet obstruction. Mol. Cell. Proteomics 17, 948–960.
Samson, G., Cardenas, D.D., 2007. Neurogenic bladder in spinal cord injury. Phys. Med. Rehabil. Clin. N. Am. 18 (255–274), vi.
Schindelin, J., Arganda-Carreras, I., Frise, E., Kaynig, V., Longair, M., Pietzsch, T., Preibisch, S., Rueden, C., Saalfeld, S., Schmid, B., Tinevez, J.-Y., White, D.J., Hartenstein, V., Eliceiri, K., Tomancak, P., Cardona, A., 2012. Fiji: an open-source platform for biological-image analysis. Nat. Methods 9, 676–682.
Schneider, M.P., Hughes Jr., F.M., Engmann, A.K., Purves, J.T., Kasper, H., Tedaldi, M., Spruill, L.S., Gullo, M., Schwab, M.E., Kessler, T.M., 2015. A novel urodynamic model for lower urinary tract assessment in awake rats. BJU Int. 115 (Suppl. 6), 8–15.
Schneider, M.P., Sartori, A.M., Ineichen, B.V., Moors, S., Engmann, A.K., Hofer, A.S., Weinmann, O., Kessler, T.M., Schwab, M.E., 2019. Anti-nogo-a antibodies as a potential causal therapy for lower urinary tract dysfunction after spinal cord injury. J. Neurosci. 39, 4066–4076.
Schöps, T.F., Schneider, M.P., Steffen, F., Ineichen, B.V., Mehnert, U., Kessler, T.M., 2015. Neurogenic lower urinary tract dysfunction (NLUTD) in patients with spinal cord injury: long-term urodynamic findings. BJU Int. 115 (Suppl. 6), 33–38.
Sie, J.A., Blok, B.F., de Weerd, H., Holstege, G., 2001. Ultrastructural evidence for direct projections from the pontine micturition center to glycine-immunoreactive neurons in the sacral dorsal gray commissure in the cat. J. Comp. Neurol. 429, 631–637.
Simpson, L.A., Eng, J.J., Hsieh, J.T., Wolfe, D.L., 2012. The health and life priorities of individuals with spinal cord injury: a systematic review. J. Neurotrauma 29, 1548–1555.
Studeny, S., Vizzard, M.A., 2005. Corticotropin-releasing factor (CRF) expression in postnatal and adult rat sacral parasympathetic nucleus (SPN). Cell Tissue Res. 322, 339–352.
Valentino, R.J., Page, M.E., Luppi, P.H., Zhu, Y., Van Bockstaele, E., Aston-Jones, G., 1994. Evidence for widespread afferents to Barrington's nucleus, a brainstem region rich in corticotropin-releasing hormone neurons. Neuroscience 62, 125–143.
Verstegen, A.M.J., Vanderhorst, V., Gray, P.A., Zeidel, M.L., Geerling, J.C., 2017. Barrington's nucleus: neuroanatomic landscape of the mouse "pontine micturition center". J. Comp. Neurol. 525, 2287–2309.
Verstegen, A.M.J., Klymko, N., Zhu, L., Mathai, J.C., Kobayashi, R., Venner, A., Ross, R. A., VanderHorst, V.G., Arrigoni, E., Geerling, J.C., Zeidel, M.L., 2019. Non-Crh glutamatergic neurons in Barrington's nucleus control micturition via glutamatergic afferents from the midbrain and hypothalamus. Curr. Biol. 29, 2775–2789.e2777.
Weld, K.J., Graney, M.J., Dmochowski, R.R., 2000. Clinical significance of detrusor sphincter dyssynergia type in patients with post-traumatic spinal cord injury. Urology 56, 565–568.
Yao, J., Li, Q., Li, X., Qin, H., Liang, S., Liao, X., Chen, X., Li, W., Yan, J., 2019. Simultaneous measurement of neuronal activity in the pontine micturition center and cystometry in freely moving mice. Front. Neurosci. 13, 663.
Zinck, N.D., Downie, J.W., 2008. IB4 afferent sprouting contributes to bladder dysfunction in spinal rats. Exp. Neurol. 213, 293–302.
Zinck, N.D., Rafuse, V.F., Downie, J.W., 2007. Sprouting of CGRP primary afferents in lumbosacral spinal cord precedes emergence of bladder activity after spinal injury. Exp. Neurol. 204, 777–790.